

**Supporting Information**

**Shape-Memory Polyurethane Foam Integrated with Nanofiber  
Technology: Synergistic Efficacy in Reducing the Risk of Capsular  
Contracture and Infection in Breast Reconstruction Applications**

*Kawun Chung<sup>a</sup>, Lunqiang Jin<sup>b\*</sup>, Qiang Zhang<sup>c</sup>, Lin Tan<sup>c</sup>, Zhenggui Du<sup>a\*</sup>*

<sup>a</sup> Department of General Surgery, Breast Center, West China Hospital, Sichuan University, Chengdu 610041, P. R. China

<sup>b</sup> Precise Synthesis and Function Development Key Laboratory of Sichuan Province, College of Chemistry and Chemical Engineering, China West Normal University, Nanchong 637002, P. R. China

<sup>c</sup> College of Biomass Science and Engineering, Key Laboratory of Biomass Fibers for Medical Care in Textile Industry, National Key Laboratory of Advanced Polymer Materials, Sichuan University, Chengdu 610065, P. R. China

\*Corresponding author: Lunqiang Jin (E-mail: jinlqchem123@163.com); Zhenggui Du (E-mail: docduzg@163.com)

### The X-ray photoelectron spectroscopy (XPS):

The XPS survey spectra of all samples reveal the presence of C, O, and N on their surfaces (**Figure S1**), consistent with the expected chemical compositions of PCL, gelatin, and polyurethane. A subtle but discernible increase in the C/O ratio is observed for PG-MA relative to PG, indicating the introduction of carbon-rich components potentially associated with magnolol modification. However, definitive confirmation of successful magnolol grafting requires further analysis of the high-resolution C 1s spectra to identify specific chemical states, particularly the contribution from aromatic carbon species

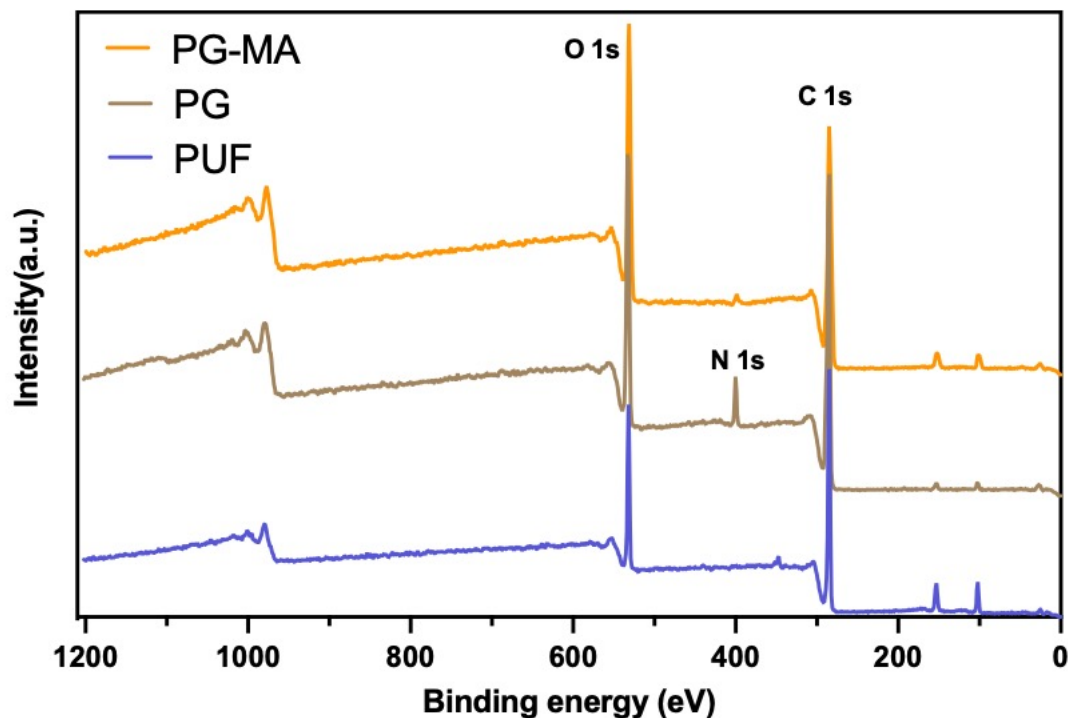


**Figure S1.** The XPS spectra of PUF, PG, and PG-MA.

### The Energy Dispersive Spectroscopy (EDS)

Energy dispersive spectroscopy (EDS, IE 3000, UK) was employed to characterize and evaluate the elemental composition. The surface elemental compositions of the PUF, PG, and PG-MA samples were analyzed by EDS. The PUF surface consisted exclusively of carbon (72.2 wt%) and oxygen (27.8 wt%) (**Figure S2A**), with no detectable nitrogen signal, consistent with its expected polymer structure lacking nitrogen-containing functional groups. The PG membrane surface exhibited carbon (67.4 wt%) and oxygen (32.6 wt%) (**Figure S2B**), while the PG-MA membrane surface was composed of carbon (68.7 wt%) and oxygen (31.3 wt%) (**Figure S2C**).

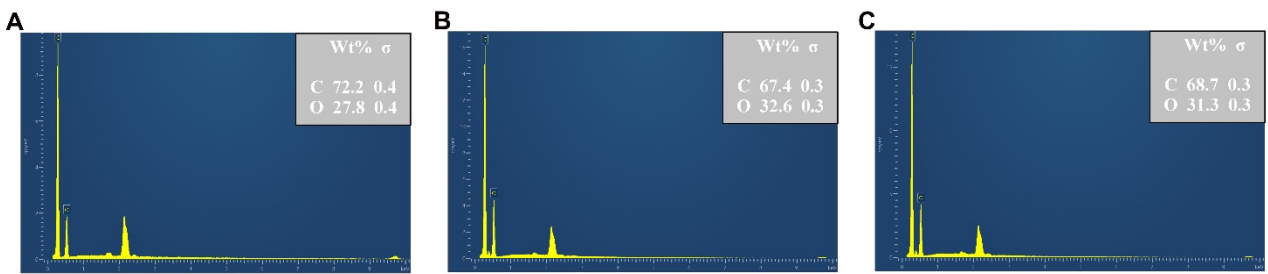


**Figure S2:** (A) Surface SEM image of PUF; EDS spectra of PUF (B), PG (C), and PG-MA.

### The standard curve

Prior to conducting drug release testing, a standard curve for drug concentration must be established. Drug standard material is accurately weighed and dissolved in phosphate-buffered saline (PBS) to prepare a high-concentration stock solution. This stock solution is then subjected to serial dilution to generate a concentration gradient ranging from 0.1 to 100  $\mu\text{g/mL}$ . Subsequently, the drug concentrations are analyzed using ultraviolet-visible (UV-Vis) spectrophotometry. Before measurement, the maximum absorption wavelength ( $\lambda_{\text{max}}$ ) of the drug is determined to be 294 nm via wavelength scanning. Each concentration level is analyzed in triplicate. The average value of the peak area or absorbance readings is plotted as the ordinate (Y-axis) against the actual concentration as the abscissa (X-axis). A linear regression equation (R) is derived using the least-squares method for curve fitting.

The resulting standard curve (**Figure S3**) will be employed for the quantitative determination of drug concentrations in subsequent drug release experiments. The fitted standard curve is deemed suitable for quantification only upon achieving a coefficient of determination ( $R^2 \geq 0.99$ ).

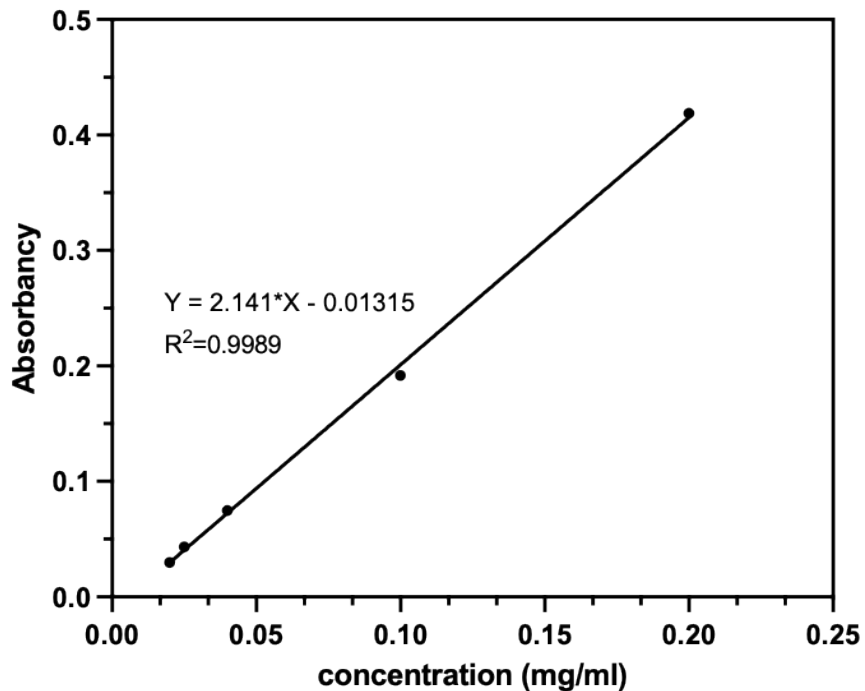


**Figure S3.** Standard curve calculations of magnolol.

### The degradation process

Degradation studies simulating physiological conditions revealed that the surface PG-Mg layer of PUF-PG-Mg composites partially or completely detached within one month, accompanied by nanofiber blurring, pore/defect formation, and eventual fracture into flake-like structures over time. Despite progressive surface PG-Mg shedding, the underlying PUF substrate maintained its porous cross-linked network integrity for at least three months.

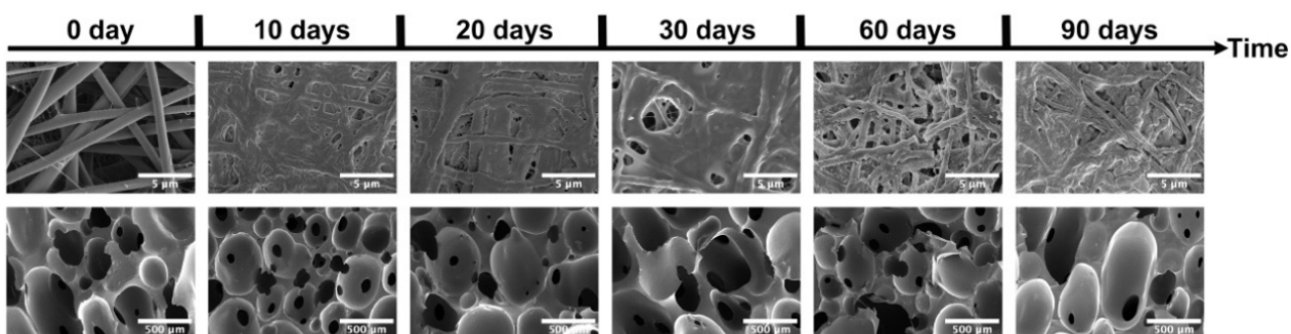


**Figure S4.** SEM images illustrating the degradation process of PUF-PG-MA.

### DMA Tensile Cycling (30 Cycles)

DMA (DMA-Q800, TA Instruments, New Castle, DE, USA) was used in tension mode to evaluate the mechanical behavior of PUF-PG-MA. Samples (10 mm × 30 mm) were subjected to cyclic tensile loading at a rate of 10 mm/min to fixed strain levels (20%, 50%) for 30 cycles. Under a tensile strain of 20% (**Figure S5A**), the material exhibited excellent elastic recovery. The stress–strain curves from 30 consecutive loading–unloading cycles showed a high degree of overlap, forming narrow and densely packed hysteresis loops, indicating minimal plastic deformation and highlighting the material’s high structural stability under low-strain cyclic loading. When the tensile strain was increased to 50% (**Figure S5B**), a distinct change in mechanical response was observed. The first cycle displayed the largest hysteresis loop and noticeable residual strain, suggesting irreversible structural rearrangements such as fiber straightening and molecular chain slippage. In subsequent cycles, the mechanical response gradually stabilized; however, the hysteresis loops remained relatively wide, reflecting sustained energy dissipation and partial plastic deformation under higher strain conditions. Quantitative analysis of the recovery ratio further supports these findings (**Figure S5C**). The recovery ratios at 20% and 50% strain were calculated to be 96.6% and 94.1%, respectively. These results demonstrate that the material exhibits predominantly elastic behavior under low-strain conditions, while retaining high recoverability even under higher strains, despite limited plastic deformation.

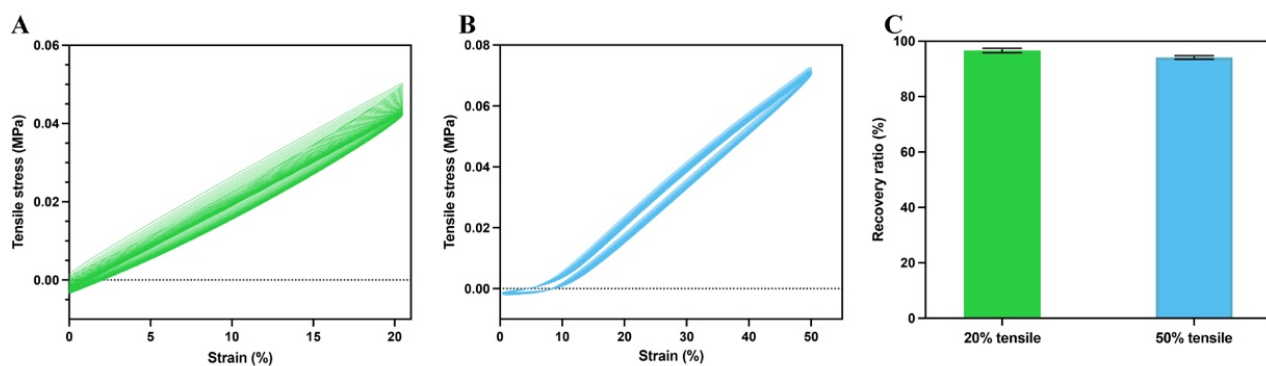


**Figure S5.** Cyclic tensile testing was performed for 30 cycles at 20% (A) and 50% strain (B); Recovery rate (%) of the PUF-PG-MA mesh after 30 cycles of tension.

### The cytocompatibility:

To elucidate the cytotoxic effects of each individual structural component within the PUF-PG-MA composite system, this experience not only assessed the integrated composite but also specifically performed cytotoxicity tests on standalone nanofibrous membranes and porous foam scaffolds,

respectively.

**Figure S6.** Cytotoxicity test of forms and membranes.

#### **Pathological comparison of the organ**

Systematic pathological evaluation of SD rats 90 days post-implantation included gross anatomical inspection and H&E staining of major organs (heart, liver, spleen, lungs, kidneys; **Figure S7**). All organs exhibited normal macroscopic features: smooth surfaces with physiological coloration (dark red cardiac tissue, homogeneous brown liver), absent calcifications, hyperplasia, or vascular anomalies. Histopathology confirmed preserved myocardial striations without interstitial edema, intact hepatic lobules with no periportal fibrosis, open splenic sinusoids, normal alveolar septa, and renal tubules devoid of protein casts or crystalline deposits. Comprehensive assessments confirmed no implant-induced organopathies, meeting biocompatibility requirements of GB/T 16886.6-2022 for medical device biological evaluation.

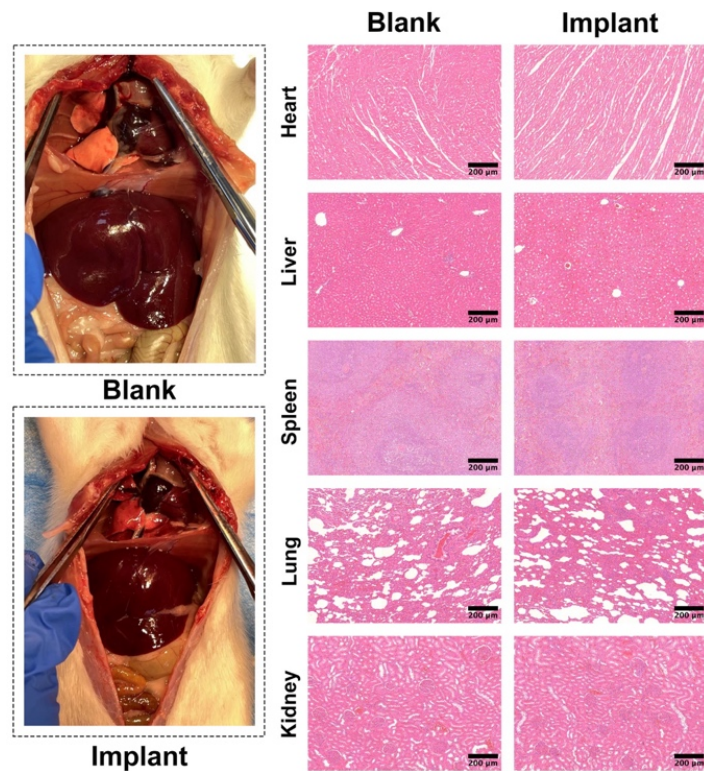


**Figure S7.** Pathological comparison of the heart, liver, spleen, lung, and kidney after 90 days of implantation.